Schaub, A-C. et al.: Brain Alterations in Individuals with Exercise Dependence: A Multimodal Neuroimaging Investigation.

https://doi.org/10.1556/2006.2024.00028

Supplementary Material

METHODS

MRI data acquisition

During the whole brain 3-dimensional T1-weighted magnetisation prepared rapid acquisition gradient (MPRAGE) sequence 224 slices were acquired with a field of view of $256mm^2$, voxels size $0.8mm^3$ isotropic spatial resolution, repetition time (RT) of 1930ms, time to echo (TE) of 2.53ms, flip angle of 8° and bandwidth of 210 Hz/pixel. The resting-state data was assessed using a gradient echo planar imaging (EPI) sequence with the following parameters: TR=3000ms, TE=28ms, slice thickness 3.0mm, field of view 256mm, flip angle 82°, 168 volumes, voxel size 3x3x3mm, bandwidth of 2326 Hz/pixel.

Structural and functional brain analysis

Structural brain analysis included an optimised VBM protocol using FSL tools. The standard and optimised VBM protocol has been validated with highly reproducible segmentation results (Douaud et al., 2007; Good et al., 2001a; Good et al., 2001b; Good et al., 2002; Maguire et al., 2000; Voets et al., 2008). First, structural images were brain extracted and grey matter segmented before being registered to the 2mm Montreal Neurological Institute (MNI) 152 standard space using nonlinear registration. Resulting images were averaged and flipped along the x-axis to create a left–right symmetric, study-specific grey matter template. Second, all native grey matter images were nonlinearly registered to this study-specific template and "modulated" to correct for local expansion (or contraction) due to the nonlinear component of the spatial transformation. An isotropic Gaussian kernel with a sigma of 3mm was used to smooth the modulated grey matter images. Outputs of each VBM step were visually checked by authors (AS). In practice, all VBM steps (except for brain extraction) did not require any manual interventions.

For pre-processing of the resting-state data, a default pipeline for volume-based analysis was applied including realignment and unwarping (subject motion estimation and correction), slice timing correction, outlier detection using ART-based identification, segmentation into grey and white matter and cerebrospinal fluid (CSF), direct normalisation into standard MNI space and smoothing (gaussian kernel FWHM=6mm) in the presented order. Denoising was done using linear regression of potential confounding effects implemented with an anatomical component-based noise correction procedure (aCompCor). It includes subject motion parameters, scrubbing (Power et al., 2014), noise components from white matter and cerebrospinal areas and session effects (constant and linear BOLD signal trends within the session) (Nieto-Castanon, 2020). Finally, linear detrending and temporal band-pass filtering ($0.0008<f<0.09$ Hz) were applied.

Statistical analysis

Group and slope comparisons

For the slope comparisons EDS scores were tested for outliers per group using Rosner test (Rosner, 1983) before analysis. In two subscales (withdrawal and continuance), two outliers were excluded. In the resting-state analysis, conn calculates brain maps of bivariate correlation coefficients (fisher transformed) for each subject and seed.

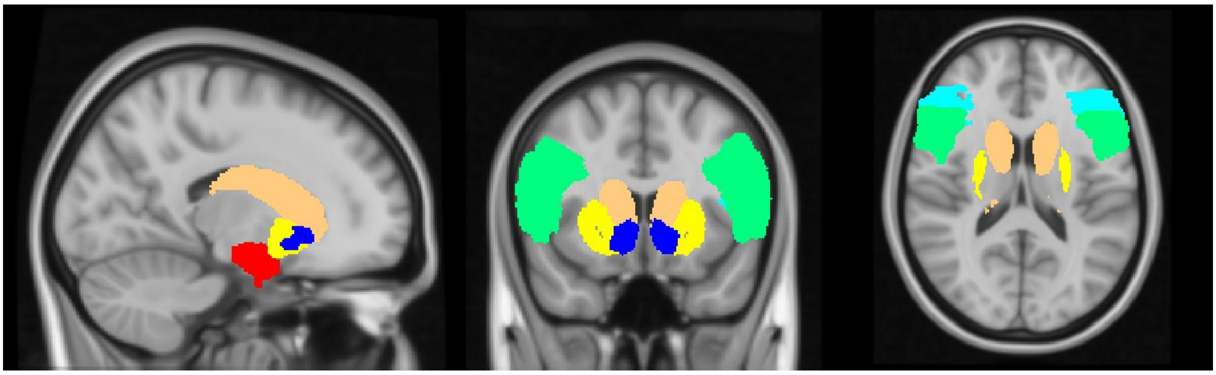

Supplementary Figure 1. Selected brain regions including bilateral amygdala (red), inferior frontal gyrus (IFG) opercularis (green), IFG triangularis (light blue), caudate (beige), putamen (yellow), nucleus accumbens (dark blue).

Supplementary References

Douaud, G., Smith, S., Jenkinson, M., Behrens, T., Johansen-Berg, H., Vickers, J., . . . James, A. (2007). Anatomically related grey and white matter abnormalities in adolescent-onset schizophrenia. *Brain, 130*, 2375-2386. doi:10.1093/brain/awm184

Good, C. D., Johnsrude, I., Ashburner, J., Henson, R. N. A., Friston, K. J., & Frackowiak, R. S. J. (2001a). Cerebral asymmetry and the effects of sex and handedness on brain structure: A voxel-based morphometric analysis of 465 normal adult human brains. *Neuroimage, 14*(3), 685-700. doi:10.1006/nimg.2001.0857

Good, C. D., Johnsrude, I. S., Ashburner, J., Henson, R. N. A., Friston, K. J., & Frackowiak, R. S. J. (2001b). A voxel-based morphometric study of ageing in 465 normal adult human brains. *Neuroimage, 14*(1), 21-36. doi:10.1006/nimg.2001.0786

Good, C. D., Scahill, R. I., Fox, N. C., Ashburner, J., Friston, K. J., Chan, D., . . . Frackowiak, R. S. J. (2002). Automatic differentiation of anatomical patterns in the human brain: Validation with studies of degenerative dementias. *Neuroimage, 17*(1), 29-46. doi:10.1006/nimg.2002.1202

Maguire, E. A., Gadian, D. G., Johnsrude, I. S., Good, C. D., Ashburner, J., Frackowiak, R. S. J., & Frith, C. D. (2000). Navigation-related structural change in the hippocampi of taxi drivers. *Proceedings of the National Academy of Sciences of the United States of America, 97*(8), 4398-4403. doi:10.1073/pnas.070039597

Nieto-Castanon, A. (2020). FMRI denoising pipeline. In *Handbook of functional connectivity Magnetic Resonance Imaging methods in CONN* (pp. 17–25): Hilbert Press.

Power, J. D., Mitra, A., Laumann, T. O., Snyder, A. Z., Schlaggar, B. L., & Petersen, S. E. (2014). Methods to detect, characterize, and remove motion artifact in resting state fMRI. *Neuroimage, 84*, 320-341. doi:10.1016/j.neuroimage.2013.08.048

Rosner, B. (1983). Percentage points for a generalized ESD many-outlier procedure. *Technometrics, 25*(2), 165-172. doi:10.2307/1268549

Voets, N. L., Hough, M. G., Douaud, G., Matthews, P. M., James, A., Winmill, L., . . . Smith, S. (2008). Evidence for abnormalities of cortical development in adolescent-onset schizophrenia. *Neuroimage, 43*(4), 665-675. doi:10.1016/j.neuroimage.2008.08.013